ELSEVIER

Benzene and aerosol production in Titan and Jupiter's atmospheres: a sensitivity study

Sébastien Lebonnois

Laboratoire de Météorologie Dynamique, IPSL, CNRS/UPMC, Box 99, F-75252 Paris Cedex 05, France

Abstract

Benzene has recently been observed in the atmosphere of Jupiter, Saturn and also Titan. This compound is required as a precursor for larger aromatic species (PAHs) that may be part of aerosol particles. Several photochemical models have tried to reproduce the observed quantities of benzene in the atmospheres of Jupiter (both low- and high-latitudes regions), Saturn and Titan. In this present work, we have conducted a sensitivity study of benzene and PAHs formation, using similar photochemical schemes both for Titan and Jupiter (low-latitudes conditions). Two different photochemical schemes are used, for which the modeled composition fairly agrees with observational constraints, both for Jupiter and Titan. Some disagreements are specific to each atmospheric case, which may point to needed improvements, especially in kinetic data involved in the corresponding chemical cycles. The observed benzene mole fraction in Titan's stratosphere is reproduced by the model, but in the case of Jupiter, low-latitudes benzene abundance is only 3% of the observed column density, which may indicate a possible influence of latitudinal transport, since abundance of benzene is much higher in auroral regions. Though, the photochemical scheme of C_6 compounds at temperature and pressure conditions of planetary atmospheres is still very uncertain. Several variations are therefore done on key reactions in benzene production. These variations show that benzene abundance is mainly sensitive to reactions that may affect the propargyl radical. The effect of aerosol production on hydrocarbons composition is also tested, as well as possible heterogenous recombination of atomic hydrogen in the case of Titan. PAHs are a major pathway for aerosol production in both models. The mass production profiles for aerosols are discussed for both Titan and Jupiter. Total production mass fluxes are roughly three times the one expected by observational constraints in both cases. Such comparative studies are useful to bring more constraints on photochemical models.
© 2005 Elsevier Ltd. All rights reserved.

Keywords: Benzene; Titan; Jupiter; Photochemistry; Aerosol production

1. Introduction

Benzene has been observed using Infrared Space Observatory (ISO) in the atmospheres of Jupiter, Saturn, and also Titan (Bézard et al., 2001a; Coustenis et al., 2003). It had already been detected in Jupiter northern polar region by IRIS/Voyager 1 (Kim et al., 1985). Photochemical modeling of the production of this compound is not fully understood yet. Moses et al. (2000) included benzene formation in their photoche-

mical model of Saturn. The level they obtain compare well with the ISO observations, though it seems to fall short by a factor of 2. Wong et al. (2000) (revised in Wong et al., 2003) studied benzene formation and the formation of heavier ring compounds in the atmosphere of Jupiter, under high-latitude conditions, with formation pathways specific to the auroral regions. In a combined study (Friedson et al., 2002), they also investigated the formation of aerosols in the polar regions, based on PAHs production. This model yields a level of benzene in the auroral region of Jupiter that is in fairly good agreement with observations of benzene in the polar region (Kim et al., 1985), but cannot explain

the level of benzene observed by ISO at mid-latitudes. For aerosol production, Wong et al. (2003) indicates that the model can match the total aerosol loading inferred in the auroral region (60°N) by Rages et al. (1999). Lebonnois et al. (2002) also included benzene in their photochemical model of Titan, and used this compound to estimate the formation of polyaromatics hydrocarbons (PAHs). In this study, the level of benzene in Titan's stratosphere was several orders of magnitude lower than the level observed by ISO, and this lead to a negligible role of the PAH pathway in the formation of aerosols. As we will show in this paper, the revision of the chemical pathway that we have made now strongly enhance the benzene level, which compares now to observation, and consequently the PAH pathway to form aerosols appears comparable to other pathways. Wilson et al. (2003) studied in detail the photochemical formation of benzene in the atmosphere of Titan. They explored the possible formation mechanisms, taking into account the large uncertainties due to lack of kinetic data. The main formation of benzene comes from recombination of propargyl radical (HC≡C-CH$_2$), and the chemical scheme they use can produce 40% of the benzene needed to account for ISO observations.

The goal of this present paper is to use the same photochemistry to study benzene and PAHs formation in the atmospheres of both Titan and Jupiter. Based first on our nominal chemical scheme, we compare the results of our models to available observations for both atmospheres. Then we test in this context the sensitivity to several reaction rates that influence benzene (and PAHs) formation. We also study the influence of the background photochemical model, using either the set of reactions used by Lebonnois et al. (2002, 2003), or the one used by Moses et al. (2000). This kind of comparative study has been done by Lee et al. (2000) to evaluate the impact on ethane and methyl abundances of uncertainties in the recombination rate of methyl radicals, using models of Titan and of the four giant planets. Comparative studies between atmospheres can help to understand the photochemistry going on in these atmospheres, and also can point the weaknesses in photochemical models.

2. Photochemical models

2.1. Photochemical schemes

Our reference set of reactions has been used in Lebonnois et al. (2002, 2003) for studies of the atmosphere of Titan. The reactions concerning benzene have been revised and are presented in Table 1 (Scheme A). For the photodissociation cross-section of benzene, we used the data published by Suto et al. (1990). The photodissociation pathways are discussed in Yokoyama et al. (1990), for wavelengths 193 and 248 nm. For many reactions in this chemical scheme, reaction rates are poorly known, especially for temperature and pressure conditions of Titan or Jupiter's atmospheres, and also for values of low-pressure limit reaction rate k_0, which are missing for some reactions. For the major productions of benzene (AR9, AR11), some estimations from previous models (Moses et al., 2000; Wilson et al., 2003) were used, and sensitivity tested. We have assumed some simplifications in our scheme:

- We consider that formation of aromatic C_6H_4 is equivalent to formation of phenyl (i.e. we assume its dominant loss is the reaction $C_6H_4 + H \rightarrow C_6H_5$), and that formation of izocyclic C_6H_7 is equivalent to formation of benzene ($C_6H_7 \rightarrow C_6H_6 + H$).
- We assume that all pathways leading to linear isomers of C_6H_6 or C_6H_7 ultimately lead to cyclisation, and therefore benzene.

The chemical scheme is therefore adapted along these assumptions. Concerning the C_6H_7 isomers, formation of benzene along reactions AR10 and AR11 ($C_2H_2 + C_4H_5$) has been discussed by Wilson et al. (2003) according to current knowledge of these pathways, at high temperatures. The dominant product of this reaction and the behavior of the C_6H_7 isomers in planetary atmospheres conditions are still uncertain, and need experimental assessment in order to better understand the role that this route may play for benzene formation in Titan or Jupiter's atmospheres.

Wilson et al. (2003) compared three different schemes, some with similar simplifications, and some with a more detailed set of compounds and reactions. The benzene profiles obtained from these schemes are very close together, suggesting that simplifying the chemical scheme in such a manner is a good approximation.

Our scheme does not include any ions or ion-neutral reactions. Wilson et al. (2003) also tested the possible role of an ionic pathway for benzene production. The conclusion seems to indicate a possible effect very high in the atmosphere (above 10 μbar), but with no significant influence on the total column abundance.

As Wilson et al. (2003) emphasised, more accurate measurements of reaction rates in the conditions of temperature and pressure corresponding to these planetary atmospheres are crucial for several key reactions, in order to fully assess the benzene cycle, and the role of PAHs in the synthesis of aerosol particles.

In order to test the sensitivity of the modeled benzene profiles to uncertainties in the chemical scheme, we have chosen some variations for the reaction rates of several reactions controlling the abundance of benzene, that will be called "key reactions" in this paper. These key reactions are the major production pathways of benzene

Table 1
Summary of reactions concerning benzene, phenyl and C_4H_5 used in scheme A. Variations used for sensitivity runs are indicated in parenthesis

	Photodissociations			Branching ratios	References
AR1	$C_6H_6 + h\nu$	$\rightarrow$	$C_6H_5 + H$	0.96	Suto et al., 1992
AR2	$C_6H_6 + h\nu$	$\rightarrow$	$CH_3 + C_5H_3$	0.04	Yokoyama et al., 1990

	Reactions			Rates	References
AR3	$H + C_4H_4$	$\rightarrow$	C_4H_5	3.32×10^{-12}	Schwanebeck and Warnatz, 1975
AR4	$H + C_4H_6$	$\rightarrow$	$C_4H_5 + H_2$	$1.05 \times 10^{-13} T^{0.7} e^{-3019/T}$	Weissman and Benson, 1988
AR5	$C_2H_2 + C_2H_3$	$\rightarrow$	C_4H_5	$4.16 \times 10^{-19} T^{1.9} e^{-1058/T}$	id.
AR6	$H_2 + C_4H_5$	$\rightarrow$	$C_4H_6 + H$	$6.61 \times 10^{-15} T^{0.5} e^{-1864/T}$	id.
AR7	$H + C_6H_5 + M$	$\rightarrow$	$C_6H_6 + M$	$k_0 = 1.82 \times 10^{28} T^{-16.3} e^{-3526/T}$	Wang and Frenklach, 1997
				$k_\infty = 1.66 \times 10^{-10}$	id.
AR8	$H + C_6H_6$	$\rightarrow$	$C_6H_5 + H_2$	$4.15 \times 10^{-10} e^{-8057/T}$	id.
AR9	$C_3H_3 + C_3H_3 + M$	$\rightarrow$	$C_6H_6 + M$	$k_0 = 6.0 \times 10^{-28} e^{1680/T}$	Estimated (Moses et al., 2000)
				$k_\infty = 1.2 \times 10^{-10}$	Morter et al., 1994
(A2R9	$C_3H_3 + C_3H_3 + M$	$\rightarrow$	$C_6H_6 + M$	$k_0 = 6.0 \times 10^{-28} e^{1680/T}$	Estimated Moses et al., 2000)
				$k_\infty = 4.0 \times 10^{-11}$	Fahr and Nayak (2000)
(A3R9	$C_3H_3 + C_3H_3$	$\rightarrow$	C_6H_6	1.2×10^{-10}	Morter et al., 1994)
AR10	$C_2H_2 + C_4H_5$	$\rightarrow$	$C_6H_6 + H$	$3.5 \times 10^{-9} T^{-1.07} e^{-2417/T}$	Wang and Frenklach, 1994
(A4R10	$C_2H_2 + C_4H_5$	$\rightarrow$	$C_6H_6 + H$	$3.16 \times 10^{-17} T^{1.47} e^{-2471/T}$	Westmoreland et al., 1989)
AR11	$C_2H_2 + C_4H_5$	$\rightarrow$	$(C_6H_7 \rightarrow) C_6H_6 + H$	$4.2 \times 10^{-19} T^{1.8} e^{-602/T}$	Weissman and Benson, 1988
(A4R11.1	$C_2H_2 + C_4H_5$	$\rightarrow$	$(C_6H_7 \rightarrow) C_6H_6 + H$	$k_= 3.3 \times 10^{-29} e^{-740/T}$	Estimated in Wilson et al., 2003
				$k_\infty = 3.25 \times 10^{-5} T^{-3.35} e^{-2638/T}$	Westmoreland et al., 1989)
(A4R11.2	$C_2H_2 + C_4H_5$	$\rightarrow$	$(n\text{-}C_6H_7 \rightarrow) C_6H_6 + H$	$k_= 3.3 \times 10^{-29} e^{-740/T}$	Estimated in Wilson et al., 2003
				$k_\infty = 1.45 \times 10^{-11} T^{-1.27} e^{-1792/T}$	Westmoreland et al., 1989)
AR12	$C_2H_3 + C_4H_3$	$\rightarrow$	C_6H_6	$4.77 \times 10^{-10} e^{-411/T}$	Duràn et al., 1988
AR13	$C_2H_3 + C_4H_5$	$\rightarrow$	$C_6H_6 + H_2$	$3.05 \times 10^{-37} T^{7.07} e^{-1817/T}$	Westmoreland et al., 1989
AR14	$C_4H_2^* + C_4H_6$	$\rightarrow$	$C_6H_6 + C_2H_2$	8.8×10^{-13}	Arrington et al., 1998; Zwier and Allen, 1996
AR15	$C_2 + C_6H_6$	$\rightarrow$	PAHs[a]	5.2×10^{-10}	Reisler et al., 1980
AR16	$C_2H + C_6H_6$	$\rightarrow$	PAHs[a]	8.2×10^{-11}	Wang and Frenklach, 1997
AR17	$C_2H_2 + C_6H_5$	$\rightarrow$	PAHs[a]	$3.72 \times 10^{-13} e^{-1561/T}$	Yu et al., 1994
(A5R18	$C_2H_2 + C_3H_3$	$\rightarrow$	$C_4H_2 + CH_3$	2.00×10^{-13}	Homann and Schweinfurth, 1981)
(A5R19	$C_2H_2 + C_3H_2$	$\rightarrow$	$C_4H_2 + CH_2$	5.00×10^{-13}	id.)

[a] These reactions are considered as the first steps of a more complex scheme leading to PAHs formation (see text, and Lebonnois et al. (2002) for details).

(AR9, AR11), its photolysis scheme, and also reactions A5R18 and A5R19, discussed below. These reactions were chosen because their rates are debated among photochemical models, but it must be kept in mind that any process affecting C_3H_3 or C_4H_5 radicals may also be a key process for benzene abundance.

The major production for benzene appears to come from the recombination of two propargyl ($HC \equiv C\text{-}CH_2$) radicals. The reaction rate for this recombination has been recently measured, but there is still debate since different studies do not agree. We adopted Morter et al. (1994) rate, which is three times higher than the rate measured by Fahr and Nayak (2000) which was favoured by Wilson et al. (2003). We also adopted the same estimation as Moses et al. (2000) for the low-pressure limit (k_0) of this reaction rate. Wilson et al. (2003) also estimated this k_0 in a similar way. In the A2 variation, we used the rate measured by Fahr and

Nayak (2000), still considering a three-body reaction, and in the A3 variation, we considered only a two-body reaction, with the rate from Morter et al. (1994).

Since there is significant uncertainties about the products and reaction rates of the $C_2H_2 + C_4H_5$ reaction (AR10, AR11), we tested (in the A4 variation simulation) another set of reaction rates (from Westmoreland et al., 1989) that was used by Wilson et al. (2003).

Apart form the benzene scheme and its variations, a significant modification has been done to our reference set of reactions. Previously, we included two reactions that had been suggested by Homann and Schweinfurth (1981):

(A5R18) $\qquad C_3H_2 + C_2H_2 \rightarrow C_4H_2 + CH_2$
(A5R19) $\qquad C_3H_3 + C_2H_2 \rightarrow C_4H_2 + CH_3$.
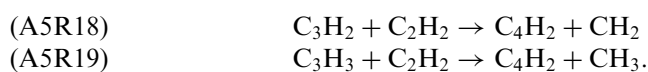
Gladstone et al. (1996) also included these reactions in their photochemical model of Jupiter. Moses et al.

(2000) argued against taking into account these reactions for their model of Saturn, based on thermodynamical data. They did include the first reaction, but with C_5H_4 as product, and estimated differently the reaction rate. Wilson et al. (2003) tested the effect of including these reactions or not. This large propargyl sink reduced their benzene level by a factor of 10^3, and they concluded that this reaction inhibiting benzene formation is not likely to take place in Titan's atmosphere. In our model, turning these reactions on or off has also a significant impact, on C_4H_2 as well as on benzene. In our nominal model, we decided not to include them. We will discuss the effects of their inclusion in Section 4.2.

We have done another small modification to our reference set of reactions: the photodissociation of C_4H_{10} has been taken into account, using Okabe and Becker (1963) for the absorption cross-sections and quantum yields of the different pathways.

The set of reactions used for Saturn by Moses et al. (2000) was also used in this study for comparison, with few adjustments: we did not include several compounds that were used in Moses et al. (2000) (different isomers of C_4H_6, C_4H_8, C_4H_9, C_6H, C_6H_2, C_6H_3, C_8H_2 and C_8H_3) and since this scheme did not include phenyl radical, we added several reactions concerning this compounds. For Titan, we also completed this scheme (that does not include any nitrogen species) with all the reactions of Scheme A involving nitrogen compounds. The reactions concerning benzene are shown in Table 2 (Scheme B).

In this scheme, the photodissociation pathways for benzene are significantly different from those used in Scheme A. We tested the influence of this difference by replacing reactions BR1-BR4 by reactions AR1-AR2 in the B2 variation simulation. Concerning the production of benzene, the dominant pathway is similar in both schemes A and B, but not the $C_2H_2 + C_4H_5$ reaction. Therefore, we also completed the A4 variation simulation with the B3 variation simulation, replacing reaction BR12 by reactions AR10 and AR11.

2.2. Photochemical models

The model we use for the atmosphere of Titan is a one-dimensional model described in Lebonnois et al. (2002, 2003), and is derived from the original model by Toublanc et al. (1995). The profile of the vertical eddy diffusion coefficient is adjusted in order to get vertical distributions of chemical compounds that are close to the profiles obtained at equator in a two-dimensional latitude–altitude model taking into account the transport of species by the general circulation in the lower atmosphere (below 500 km, i.e. below the 1-μbar level)

(Lebonnois et al., 2001). We consider annual mean equatorial conditions.

For the atmosphere of Jupiter, we use a one-dimensional model very similar to the one published by Gladstone et al. (1996), for annual mean equatorial conditions. Since our goal is not to explore in depth the composition of Jupiter's atmosphere, nor to study effects of various small details in the modeling, we chose to adopt several approximations in order to keep the model simple, while getting results close to those obtained by Gladstone et al. (1996). We use the pressure and temperature profiles prescribed in this model for the North Equatorial Belt (NEB, 10°N). Altitude range considered is -50 km ($p = 5$ bar) to 600 km ($p = 10^{-6}$ mbar), with the reference altitude level ($z = 0$) fixed at $p = 1$ bar. The vertical eddy diffusion coefficient profile is also taken for the NEB conditions: $K(n) = K_H((n - H)/n)^\gamma$ for $p \lesssim p_T$, and $K(n) = K_T$ for $p \gtrsim p_T$, where n is the density, H refers to the homopause level ($p_H = 0.1$ μbar, $K_H = 1.4 \times 10^3$ cm^2 s^{-1}, $n_H = 1.4 \times 10^{13}$ cm^{-3}), T refers to the tropopause level ($p_T = 100$ mbar, $K_T = 10^3$ cm^2 s^{-1}), and $\gamma = 0.45$. The molecular diffusion coefficients are obtained with the same formula as in Eq. (6) of Gladstone et al. (1996). Mean molecular mass is held constant at 2.25 amu. Mixing ratio of helium is fixed to 0.11. The ultraviolet actinic flux is calculated for wavelengths between 10 and 310 nm, using simple absorption of the incident beam in a plane-parallel atmosphere. This calculation is done interactively with the calculation of the photochemistry. In the same way as the Gladstone et al. (1996) model, we neglect effects of Rayleigh and aerosols scattering, and absorption by NH_3. These approximations induce errors in the actinic fluxes below the tropopause, so caution should be taken with the resulting tropospheric composition. At the upper boundary, a downward flux of hydrogen atoms of 4×10^9 cm^{-2} s^{-1} is taken into account. This flux results from the production of atomic hydrogen in the thermosphere by various processes resulting from the absorption of solar EUV radiation by H_2 (Gladstone et al., 1996). At the lower boundary, the mixing ratios of methane is fixed to 2.2×10^{-3}. For compounds other than molecular hydrogen, helium and methane, the downward flux is estimated in the same way as in the Gladstone et al. (1996) model.

The production of aerosols by photochemistry is estimated in both Titan and Jupiter's atmospheres using the same parameterization, as described in Lebonnois et al. (2002).

All three pathways are used in the case of Titan: polymers of acetylene and cyanoacetylene, polycyclic aromatic hydrocarbons (PAHs) that may include nitrogen atoms, and polymers of nitriles (mainly HCN). Concerning the PAHs, the initial reactions leading to the formation of macromolecules are reactions AR15, AR16 and AR17 for scheme A, and BR16 for scheme

Table 2
Similar to Table 1, but for scheme B

	Photodissociations			Branching ratios	References[a]
BR1	$C_6H_6 + h\nu$	→	$C_6H_5 + H$	0.10	Pantos et al., 1978
BR2	$C_6H_6 + h\nu$	→	$3C_2H_2$	0.84	Malkin, 1992
BR3	$C_6H_6 + h\nu$	→	$C_2H_4 + C_4H_2$	0.05	
BR4	$C_6H_6 + h\nu$	→	$2C_3H_3$	0.01	
(B2R1	$C_6H_6 + h\nu$	→	$C_6H_5 + H$	0.96	Suto et al., 1992)
(B2R2	$C_6H_6 + h\nu$	→	$CH_3 + C_5H_3$	0.04	Yokoyama et al., 1990)

	Reactions			Rates	References[a]
BR5	$H + C_4H_4 + M$	→	$C_4H_5 + M$	$k_0 = 6.0 \times 10^{-31} e^{1680/T}$	Estimated
				$k_\infty = 3.32 \times 10^{-12}$	Schwanebeck et al., 1975
BR6	$H + C_4H_5$	→	$C_4H_4 + H_2$	2.0×10^{-11}	Estimated
BR7	$H + C_4H_5 + M$	→	$C_4H_6 + M$	$k_0 = 6.0 \times 10^{-30} e^{1680/T}$	id.
				$k_\infty = 1.0 \times 10^{-10}$	Gladstone et al., 1996
BR8	$H_2 + C_4H_5$	→	$C_4H_6 + H$	$6.61 \times 10^{-15} T^{0.5} e^{-1864/T}$	Weissman and Benson, 1988
BR9	$CH_3 + C_4H_5$	→	$C_4H_4 + CH_4$	3.4×10^{-11}	Estimated
BR10	$CH_3 + C_4H_5 + M$	→	products $+ M$	$k_0 = 7.12 \times 10^{-22} e^{715/T}$ ($T \leqslant 200$ K)	id.
				$k_0 = 4.57 \times 10^{-24} e^{2184/T}$ ($T > 200$ K)	id.
				$k_\infty = 3.2 \times 10^{-10} T^{-0.32}$	id.
BR11	$C_2H_2 + C_2H_3 + M$	→	$C_4H_5 + M$	$k_0 = 8.2 \times 10^{-30} e^{-352/T}$	id.
				$k_\infty = 4.16 \times 10^{-19} T^{1.9} e^{-1058/T}$	Weissman and Benson, 1988
BR12	$C_2H_2 + C_4H_5$	→	$C_6H_6 + H$	$3.16 \times 10^{-17} T^{1.47} e^{-2471/T}$	Westmoreland et al., 1989
(B3R12.1	$C_2H_2 + C_4H_5$	→	$C_6H_6 + H$	$3.5 \times 10^{-9} T^{-1.07} e^{-2417/T}$	Wang and Frenklach, 1994)
(B3R12.2	$C_2H_2 + C_4H_5$	→	$(C_6H_7 \rightarrow)C_6H_6 + H$	$4.2 \times 10^{-19} T^{1.8} e^{-602/T}$	Weissman and Benson, 1988)
BR13	$C_3H_3 + C_3H_3 + M$	→	$C_6H_6 + M$	$k_0 = 6.0 \times 10^{-28} e^{1680/T}$	Estimated
				$k_\infty = 1.2 \times 10^{-10}$	Morter et al., 1994
BR14[b]	$H + C_6H_5 + M$	→	$C_6H_6 + M$	$k_0 = 1.82 \times 10^{28} T^{-16.3} e^{-3526/T}$	Wang and Frenklach, 1997
				$k_\infty = 1.66 \times 10^{-10}$	id.
BR15[b]	$H + C_6H_6$	→	$C_6H_5 + H_2$	$4.15 \times 10^{-10} e^{-8057/T}$	id.
BR16[b]	$C_2H_2 + C_6H_5$	→	PAHs[c]	$3.72 \times 10^{-13} e^{-1561/T}$	Yu et al., 1994

[a]This scheme is essentially taken from Moses et al. (2000), with references and estimations. Details for these estimations should be looked for in Moses et al. (2000).

[b]Reactions concerning phenyl radical were added from scheme A, since this radical was not considered in Moses et al. (2000).

[c]Same remark as for AR15-17.

B. The other parameters are similar to those described in Lebonnois et al. (2002), especially the mean length of the polymers $N_i = 20$. This parameter represents the mean number of gas phase molecules (C_2H_2, HCN, HC_3N) that are added together in one single polymer macromolecule, and may range from 10 to 100. The chosen value corresponds to approximately 10 macromolecules in a haze particle of radius around 10 Å.

In the case of Jupiter, no nitriles are included, so the pathways are reduced to aliphatic polymers of acetylene, and PAHs. Initial reactions are the same as in the case of Titan (same chemical schemes), and we kept also the mean length of the polymers to $N_i = 20$, though more constraints are needed to better adjust this parameter.

3. Simulations

Simulations are labelled using a code to identify the atmosphere and the chemistry considered. This code starts with T for Titan or J for Jupiter. Then the chemical scheme is indicated as in Tables 1 and 2: A1/B1 for the nominal chemical scheme A/B, An/Bn for the variations on indicated reactions. There is then a suffix 'a' when the aerosol production scheme is on. A suffix 'b' is added when the heterogenous recombination of atomic hydrogen is also taken into account (together with aerosol production), as described in Lebonnois et al. (2003), which is only done for Titan's atmosphere. Therefore, our reference simulations for Titan are TA1 (no aerosol production) and TA1a (with aerosol production), and JA1 or JA1a for Jupiter.

All simulations have been run for 5 planetary years (which is a total of 1.87×10^9 s for Jupiter and 4.73×10^9 s for Titan), starting from the same atmospheric initial composition. Residual variations at the end of each simulation are less or of the order of 10^{-4}.

4. Results

4.1. Comparison to observations

4.1.1. Titan
Observational constraints have been obtained for Titan's atmospheric composition from:

- Voyager 1/IRIS spectra (Coustenis et al., 1989, 1991; Coustenis and Bézard, 1995), which constrained the stratospheric composition for several latitudes, at northern spring equinox;
- Infrared Space Observatory (ISO) spectra (Coustenis et al., 2003), which are disk averaged (and are therefore essentially representative of equator and mid-latitudes) for mid-northern autumn;
- the reanalysis of Voyager 1/UVS spectra (Vervack, 1997), which constrained composition in the 500–800 km altitude range, but have not yet been confirmed;
- from millimeter wavelengths ground-based observations (Marten et al., 2002), which are disk-averaged, and constrained nitriles stratospheric profiles also for mid-northern autumn.

In Fig. 1, vertical profiles of hydrocarbons observed in Titan's atmosphere are displayed for our reference simulation (TA1) and for simulations using chemical scheme B (TB1 and TB2, depending on the photodissociation scheme used for benzene), and compared with stratospheric constraints from IRIS/Voyager 1 and ISO spectra. The comparison between models and observations is similar to previously published results. As in previous papers related to photochemical modeling of Titan's atmosphere, ethylene is clearly underestimated in any case (Toublanc et al., 1995; Lara et al., 1996; Lebonnois et al., 2001). Other compounds are in fairly good agreement with observations. Differences between schemes A and B are mainly visible for benzene, but also for diacetylene, for which scheme A seems in better agreement than scheme B, and also for methylacetylene in the upper atmosphere.

4.1.2. Jupiter
Observational constraints for Jupiter's atmosphere have been obtained from Voyager 1/IRIS spectra, and also recently from ISO spectra. The constraints used in Fig. 2 and Table 3 have been compiled from Gladstone et al. (1996), Atreya et al. (1999, 2003), Bézard et al. (2001a,b), Fouchet et al. (2000), and references therein.

Vertical profiles of hydrocarbons for Jupiter's atmosphere are displayed for our reference simulation (JA1) and for simulations using chemical scheme B (JB1 and JB2) in Fig. 2. Comparison is also done between these simulations and observational constraints on column
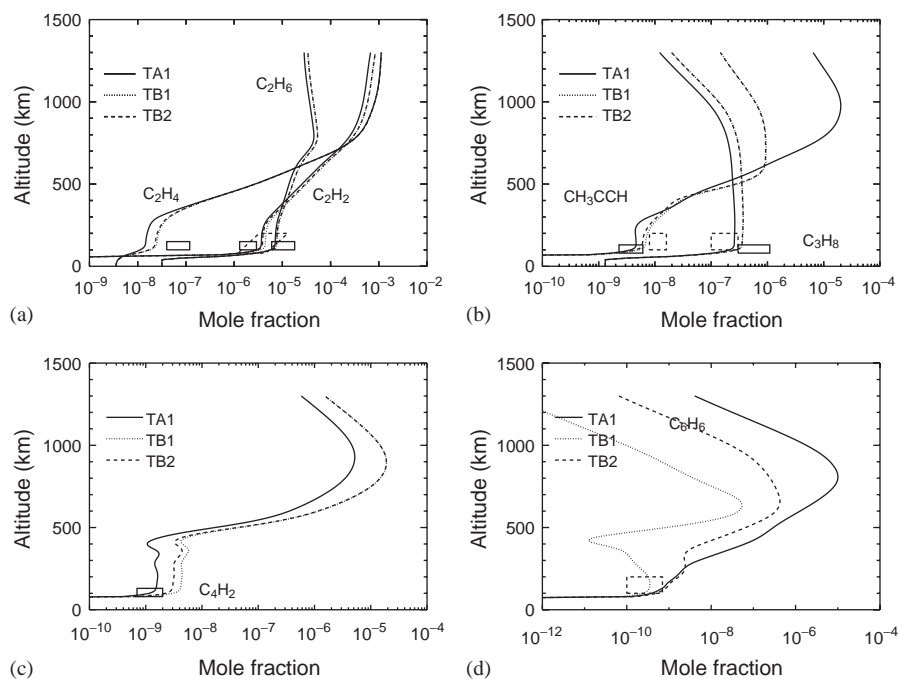

Fig. 1. Comparison between vertical profiles in Titan's atmosphere from simulations TA1, TB1 and TB2. (a) Acetylene (C_2H_2), ethylene (C_2H_4) and ethane (C_2H_6); (b) methylacetylene (CH_3C_2H) and propane (C_3H_8); (c) diacetylene (C_4H_2); (d) benzene (C_6H_6). The boxes represent observational constraints obtained from Coustenis and Bézard, 1995 (solid line boxes, IRIS/Voyager 1) and from Coustenis et al. (2003) (dashed line boxes, ISO).
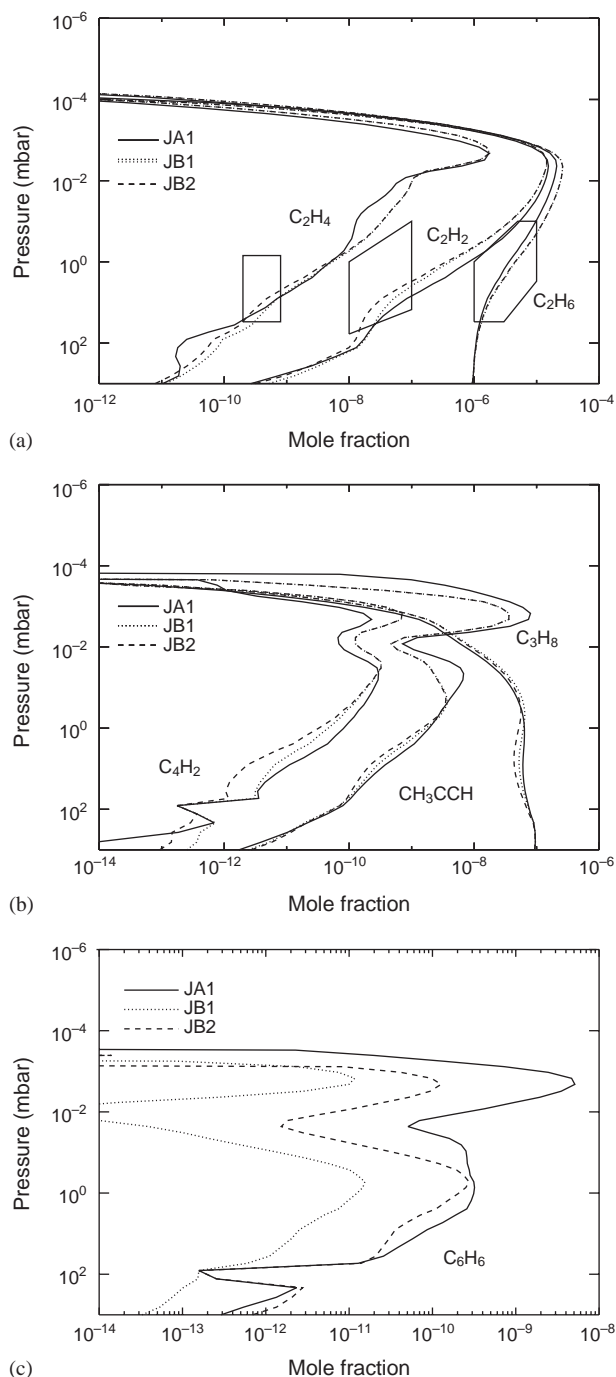
(a)

(b)

(c)

Fig. 2. Comparison between vertical profiles in Jupiter's atmosphere from simulations JA1, JB1 and JB2. (a) acetylene, ethylene and ethane; (b) methylacetylene, propane and diacetylene; (c) benzene. The boxes represent observational constraints compiled from Gladstone et al. (1996), Atreya et al. (1999, 2003), Bézard et al. (2001a,b), Fouchet et al. (2000), and references therein.

Table 3
Comparison between simulations and observational constraints for several hydrocarbons in Jupiter's atmosphere

Species	Column densities in cm^{-2}			
	JA1	JB1	JB2	Observations
C_2H_4	6.7×10^{14}	1.0×10^{15}	7.6×10^{14}	2–3×10^{15}[a]
CH_3C_2H	3.6×10^{14}	3.2×10^{14}	3.1×10^{14}	1.5×10^{15}[b]
C_4H_2	8.6×10^{12}	9.7×10^{12}	4.6×10^{12}	$<7 \times 10^{13}$[b]
C_6H_6 (p < 50 mbar)	3.2×10^{13}	1.1×10^{12}	1.8×10^{13}	$\sim 9 \times 10^{14}$[c]

[a]Bézard et al. (2001b).
[b]Fouchet et al. (2000).
[c]Bézard et al. (2001a).

agreement with observations, though the total column density of ethylene is underestimated. The total column density of methylacetylene is underestimated by a factor of 5. For benzene, all models largely underestimate the column density. In the JA1 simulation, the column density represents only 3% of what is required by the observations.

4.2. Influence of the uncertainties on key reactions

4.2.1. Variation in the photolysis pathways

Comparing the simulations B1 and B2 (both for Titan and Jupiter) can highlight the main differences between the two different photodissociation schemes for benzene. Most hydrocarbons and nitriles are not affected by the selected scheme. Benzene and phenyl are almost the only species that really show different vertical profiles between simulations B2 and B1, though C4H2 is also affected, being increased by 35 percent in B1, compared to B2 in the stratosphere of Titan, and up to a factor of 3 in the stratosphere of Jupiter. The different profiles of benzene are shown in Figs. 1d and 2c.

Though benzene in simulation TB1 may be in better agreement with the estimation from ISO observations in the atmosphere of Titan than in simulation TB2 (where it appears to be slightly overestimated), it is reversed in Jupiter's simulations, since in JB2 (and JA1), benzene is already underestimated. It is therefore difficult to conclude about photodissociation scheme on the basis of comparison to available observations.

4.2.2. Variation in the rate of the key production of benzene

A2 and A3 variations simulations concern the main production pathway for benzene, that is propargyl recombination. Almost no differences can be noticed between A1, A2 and A3 simulations, both for Titan and for Jupiter, for most of the constituents of the atmospheres. As far as benzene and propargyl are concerned, a slight variation is visible, with a 20–50 percent increase

densities in Table 3. As in the case of Titan, acetylene, ethane and diacetylene are in fairly good agreement with observations. For the other compounds, there are qualitative differences between the case of Jupiter and the case of Titan. Ethylene's vertical profile is in good

of benzene with the Morter et al. (1994) rate, and a 30–40 percent decrease of propargyl.

The effect of using two- instead of three-body reaction rates (A3, compared to A1) is only visible for benzene and propargyl above $\sim 1 \times 10^{-4}$ mbar on Titan (600–700 km altitude), and $\sim 1 \times 10^{-2}$ mbar on Jupiter. Benzene is then increased in the upper atmosphere in the A3 simulation.

4.2.3. Variation in the rate of $C_2H_2 + C_4H_5$

In both schemes, variations simulations concerning the rate of the reaction between acetylene and C_4H_5 (i.e. A4 and B3) did not display any significant variations on any compound's profile, neither on Jupiter nor on Titan. This is consistent with the fact that this production pathway for benzene is only secondary. It must also be kept in mind that this pathway, involving C_6H_7 isomers, is uncertain and has not been assessed in the temperature and pressure conditions of planetary atmospheres.

4.2.4. Impact of the introduction of reactions between acetylene and C_3H_2 or C_3H_3

Introducing these two reactions in the photochemical scheme A was tested in the A5 variation. It has no impact on C_2 species. It essentially affects the chemical cycles of C_4H_2 (with a significant additional production), C_3H_3 (dominant loss), C_3H_4 (both isomers, linked to C_4H_2 and C_3H_3 cycles), and benzene (through recombination of C_3H_3). These effects are plotted on Fig. 3. With these reactions, diacetylene is increased by a factor of approximately 4 in Titan's stratosphere, and a factor of 3 to 100 in the atmosphere of Jupiter,

depending on altitude, with a column density increasing from 8.6×10^{12} to 4.4×10^{14} cm^{-2}. For C_3H_4, the effect is reversed, with similar factors. Propargyl undergoes a strong decrease due to the significant additional loss induced by these reactions, by approximately two orders of magnitude in both stratospheres. But in response, benzene only decreases by factors around 2–3 for Titan and around 10 for Jupiter. This decrease is less pronounced than the one of C_3H_3, which seems to indicate that the other production pathways become dominant. It is significantly different from the result obtained by Wilson et al. (2003), where the decrease in benzene's mole fraction reached 3 orders of magnitude when these two reactions were added to the chemical scheme.

Taking into account these reactions worsen the fit for diacetylene, methylacetylene and benzene mole fractions in the stratosphere for both Titan and Jupiter. Until further improvement in the measure of the reaction rate and products of these reactions, it seems more reasonable not to include them in the chemical scheme.

4.3. Influence of aerosol production

For Titan, including the aerosol production has some impact on the stratospheric mole fraction for most hydrocarbons and nitriles, as it was shown by Lebonnois et al. (2002). In Fig. 4, the variations of some hydrocarbons profiles are indicated for TA1 and TA1a simulations. Variations in the cases TB1 and TB2 are very similar. In the case of Jupiter, the variations
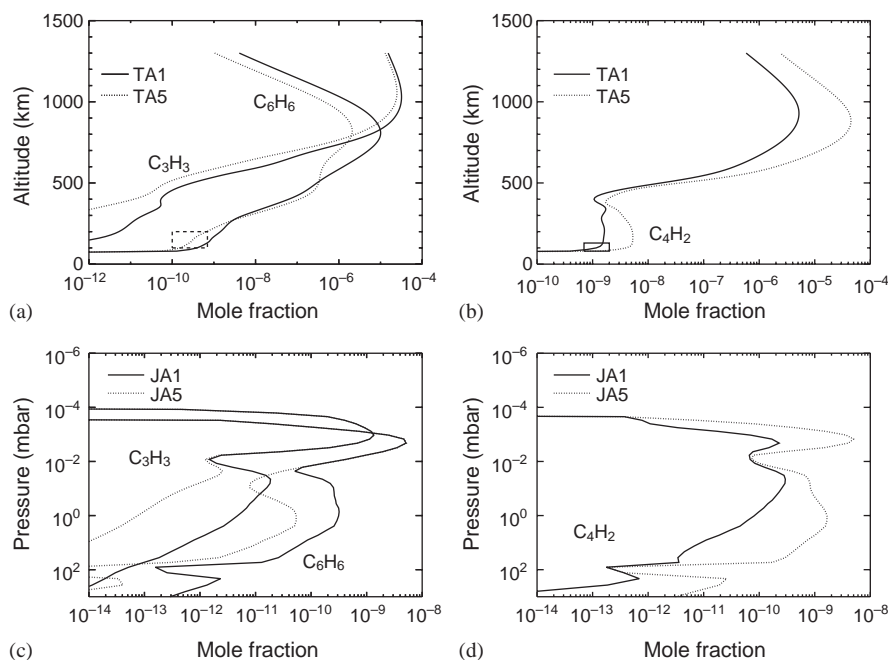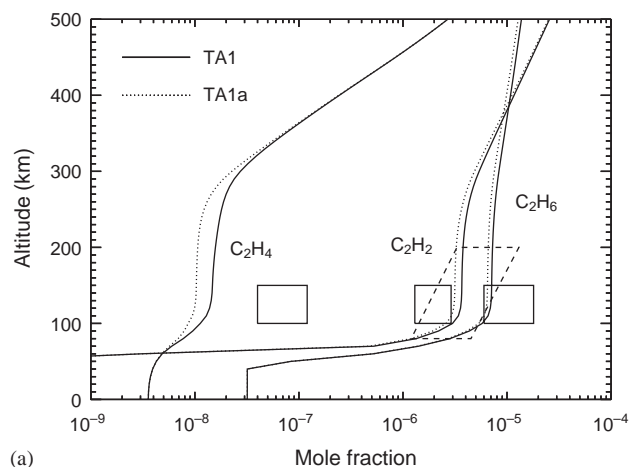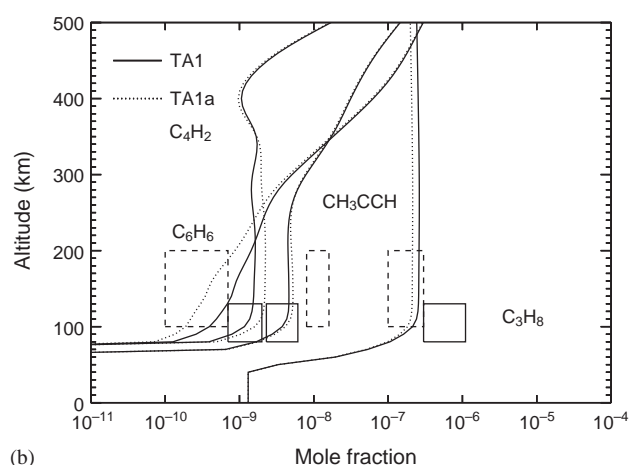

Fig. 3. Comparison between vertical profiles of propargyl radical (C_3H_3), benzene and diacetylene: (a,b) in Titan's atmosphere from simulations TA1 and TA5; (c,d) in Jupiter's atmosphere from simulations JA1 and JA5.
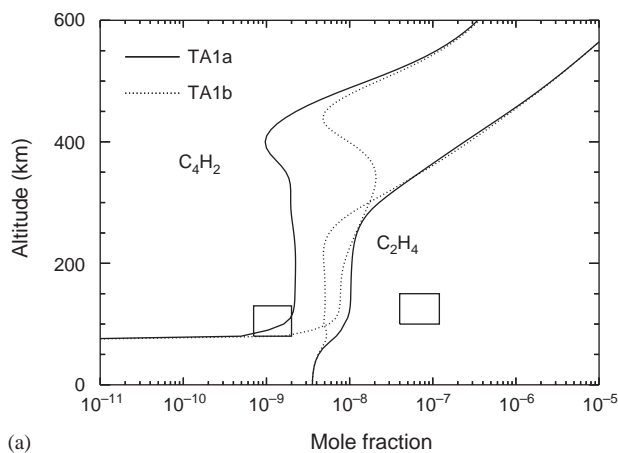
Fig. 4. Influence of the aerosol production scheme in Titan's atmosphere. Comparison between vertical profiles in Titan's atmosphere from simulations TA1 and TA1a. (a) Acetylene, ethylene and ethane; (b) methylacetylene, propane, diacetylene and benzene.

Fig. 5. Influence of the heterogenous recombination of atomic hydrogen in Titan's atmosphere. Comparison between vertical profiles in Titan's atmosphere from simulations TA1a and TA1b. (a) Diacetylene and ethylene; (b) methylacetylene and benzene.

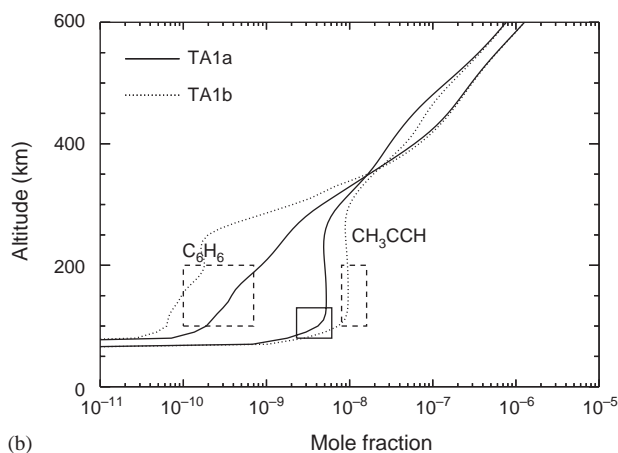between simulations with or without aerosol production are negligible.

4.4. Influence of heterogenous recombination of H (for Titan)

As it was discussed in Lebonnois et al. (2003), the main effect of this heterogenous process is to reduce the mole fraction of atomic hydrogen in the region 200–400 km of altitude. This reduction has consequences on the chemical equilibrium in this region. In the present scheme A1, Fig. 5 shows how ethylene, methylacetylene, diacetylene and benzene are affected. In scheme B1, variations are very similar, except for CH_3C_2H, for which the variation is reversed.

As far as comparison to observational constraints is concerned, there is not much difference between simulations TA1a and TA1b. Only in the case of diacetylene is the fit to observations deteriorated when the heterogenous process is taken into account.

5. Discussion

5.1. Benzene

These sensitivity studies around the photochemical scheme show that crossing the analysis between models of different atmospheres can bring new informations. Scheme A1 produces more benzene than scheme B1: it appears better in the case of Jupiter since even in simulation JA1, benzene production is still underestimated; but in the case of Titan, simulation TB1 may be closer to observations. Taking into account the aerosol production improves the fit in simulation TA1a, and does not affect the Jupiter simulations. This tends to favor scheme A1 over scheme B1.

Concerning the production pathways of benzene, this work indicates that the uncertainties linked to chemical rates and chemical pathways discussed here are not of major significance. Only the possible reaction between propargyl radical and acetylene affects benzene (and

other hydrocarbons) significantly. Though, it is certainly necessary to better understand the photochemical scheme of C_6 compounds at temperature and pressure conditions of planetary atmospheres.

In the case of Jupiter's high-latitudes conditions, observations indicate an enrichment in the auroral regions compared to low-latitudes (Kim et al., 1985; Bézard et al., 2001a). Works by Wong and colleagues (Wong et al., 2000, 2003) have shown that the energy input from auroras and specific ion chemistry can produce enough benzene to match the observations in this region. The case of Titan may indicate that the neutral chemical schemes for benzene production are understood in first approximation. The underestimation of benzene in Jupiter's low latitudes might then indicate the need for additional processes, e.g. meridional transport.

5.2. Aerosol production

As indicated previously, the mass production profiles of different pathways for aerosols formation has been evaluated in a similar way as in Lebonnois et al. (2002). For Titan, these pathways include aliphatic polymers of acetylene and cyanoacetylene, PAHs (including nitrogen), and nitriles polymers. For Jupiter, only aliphatic polymers of acetylene and PAHs are considered.

Concerning Titan, the results are similar to those obtained previously (Lebonnois et al., 2002), except for the PAHs (see Fig. 6a). Benzene was strongly underestimated in this previous work, resulting in a negligible role of PAHs in the total aerosol production. In the present work, benzene mole fraction is consistent with the analysis of the ISO spectra, and the PAHs pathway is therefore comparable to the other two pathways. The PAHs/aliphatics ratio in the precursors is of the order of unity. But it must be kept in mind that the C_6 chemical scheme is still uncertain for a large part, and that there may be exchanges between aliphatics and aromatics that are not taken into account here. As an example, the product of the reaction between C_2H_2 and C_4H_3 is n-C_6H_5 in this scheme, and is the source of the aliphatic pathway. Whether this product is aliphatic or not is still uncertain, and also there may be partial cyclisation of n-C_6H_5 and therefore exchanges between the two C_6H_5 isomers.

For Jupiter, the PAHs production is dominant over the aliphatic pathway, as seen in Fig. 6b. The remark concerning possible exchanges between the two pathways is also valid here. For low-latitudes conditions ($9°$), Rages et al. (1999) have analyzed high phase angle Galileo images of Jupiter's limb, and the corresponding haze model indicates a sedimentary flux of $6–9 \times 10^{-16}\,\mathrm{g\,cm^{-2}\,s^{-1}}$. The total production rate obtained with our aerosol production scheme ($2.8 \times 10^{-15}\,\mathrm{g\,cm^{-2}\,s^{-1}}$) is a factor of approximately 3 higher
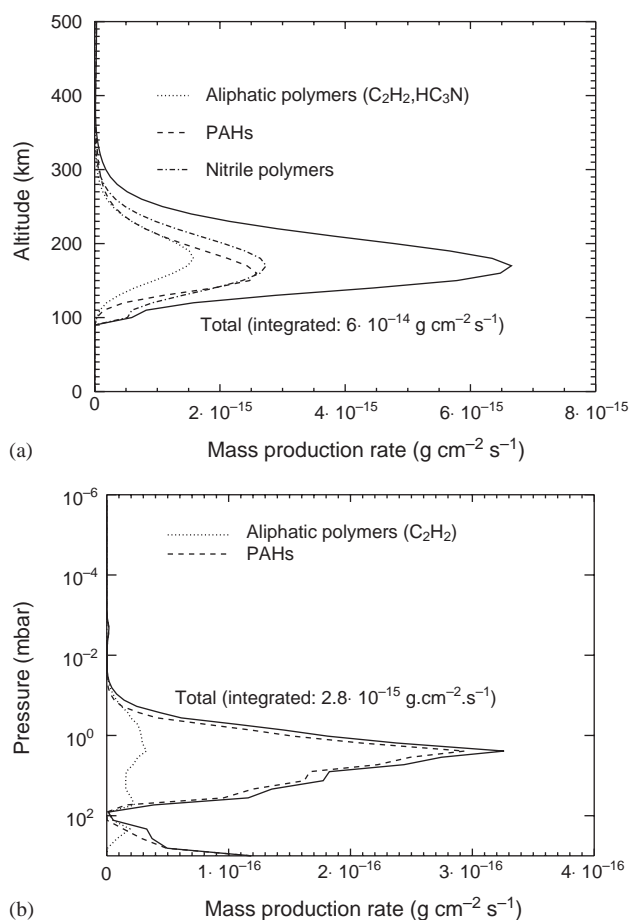

Fig. 6. Vertical profiles of the mass production rates of polymers obtained from the aerosol production scheme (a) for Titan's atmosphere (simulation TA1a); (b) for Jupiter's atmosphere (simulation JA1a).

than that modeled sedimentary flux. This quantitative comparison is consistent with the comparison between model and microphysical constraints for the atmosphere of Titan. The altitude of the haze production peak seen in Fig. 6b is located just below the 1-mbar level. We plan to couple these production profiles with a microphysical model, in order to test the resulting aerosol layer against constraints obtained from observations of Jupiter by Voyager, Galileo and the Hubble Space Telescope.

6. Conclusion

In this work, we have used the same photochemical schemes in photochemical models of both Titan and Jupiter (in low-latitudes conditions). Two schemes were used, one (scheme A) based on the set of reactions used by Lebonnois et al. (2001, 2002, 2003), the other (scheme B) based on the set of reactions published for Saturn by Moses et al. (2000). These are neutral schemes, and therefore do not apply to Jupiter polar regions, for

which auroral effects are dominant in the formation of benzene. In the photochemical scheme of C_6 species, some simplifications were done, which are in agreement with a recent work on benzene formation in the atmosphere of Titan (Wilson et al., 2003). Some sensitivity studies have been done for several key reactions in the benzene scheme.

The main results of this study are the following:

- Agreement with available observations is fairly good for most hydrocarbons. Some disagreements are specific to one atmospheric case or the other: ethylene stratospheric mole fraction is underestimated by roughly an order of magnitude for Titan but not for Jupiter, though the total column density is underestimated by a factor of 3–4; methylacetylene total column density is underestimated by a factor of 5 in Jupiter's atmosphere but its stratospheric mole fraction is in good agreement in the case of Titan.
- The observed stratospheric mole fraction of benzene in Titan is reproduced by the photochemical model. In the case of Jupiter, the model produces only 3% of the required column density. Since in Jupiter auroral regions, benzene level is much higher than at low latitudes, this might indicate a possible role of meridional transport.
- Scheme A and B produce very similar results for most hydrocarbons. Differences are visible for benzene, diacetylene and methylacetylene. Taking into account the aerosol production scheme, scheme A appears to produce slightly better results than scheme B.
- The sensitivity studies done for several key reactions in benzene's production scheme show that the uncertainties discussed here are not of first order significance. Only the possible reaction between propargyl radical and acetylene affects benzene (and other hydrocarbons) significantly.
- Taking into account aerosol production does not affect significantly the comparisons with observations. In the case of Titan, taking into account the heterogenous recombination of atomic hydrogen or not is also very similar, except that it deteriorates the fit for diacetylene, increasing its stratospheric level by a factor of 4.
- The PAHs production is a major pathway for aerosol production given the level of benzene in Titan and Jupiter's atmospheres. In Titan, it compares with aliphatic acetylene/cyanoacetylene polymers, and nitriles polymers. It is the dominant aerosol production in the case of Jupiter (as far as NH_3 photochemistry is not taken into account). It must be kept in mind that there may be exchange possibilities between aliphatic acetylene polymers and PAHs that are not taken into account in the model used here, due to the uncertainties in the C_6 scheme. The total aerosol production mass flux is roughly 3 times the one expected by observational constraints for both Titan and Jupiter.

Such comparative studies are useful to bring more constraints on photochemical models, and may help to locate difficulties in the chemical schemes. Further studies should also include Saturn.

References

Arrington, C.A., Ramos, C., Robinson, A.D., Zwier, T.S., 1998. Aromatic ring-forming reactions of metastable diacetylene with 1,3-butadiene. J. Phys. Chem. A 102, 3315–3322.

Atreya, S.K., Mahaffy, P.R., Niemann, H.B., Wong, M.H., Owen, T.C., 2003. Composition and origin of the atmosphere of Jupiter—an update, and implications for the extrasolar giant planets. Planet. & Space Sci. 51, 105–112.

Atreya, S.K., Wong, M.H., Owen, T.C., Mahaffy, P.R., Niemann, H.B., de Pater, I., et al., 1999. A comparison of the atmospheres of Jupiter and Saturn: deep atmospheric composition, cloud structure, vertical mixing, and origin. Planet. & Space Sci. 47, 1243–1262.

Bézard, B., Drossart, P., Encrenaz, T., Feuchtgruber, H., 2001a. Benzene on the giant planets. Icarus 154, 492–500.

Bézard, B., Moses, J.I., Lacy, T., Greathouse, T., Richter, M., Griffith, C., 2001b. Detection of ethylene (C_2H_4) on Jupiter and Saturn in non-auroral regions. B.A.A.S. 33, 1079.

Coustenis, A., Bézard, B., 1995. Titan's atmosphere from Voyager infrared observations. IV. Latitudinal variations of temperature and composition. Icarus 115, 126–140.

Coustenis, A., Bézard, B., Gautier, D., 1989. Titan's atmosphere from Voyager infrared observations. I. The gas composition of Titan's equatorial region. Icarus 80, 54–76.

Coustenis, A., Bézard, B., Gautier, D., Marten, A., Samuelson, R., 1991. Titan's atmosphere from Voyager infrared observations. III. Vertical distributions of hydrocarbons and nitriles near Titan's north pole. Icarus 89, 152–167.

Coustenis, A., Salama, A., Schulz, B., Ott, S., Lellouch, E., Encrenaz, T., Gautier, D., Feuchtgruber, H., 2003. Titan's atmosphere from ISO mid-infrared spectroscopy. Icarus 161, 383–403.

Duràn, R.P., Amorebieta, V.T., Colussi, A.J., 1988. Is the homogeneous thermal dimerization of acetylene a free-radical chain reaction? Kinetic and thermochemical analysis. J. Phys. Chem. 92, 636–640.

Fahr, A., Nayak, A., 2000. Kinetics and products of propargyl (C_3H_3) radical self-reactions and propargyl-methyl cross-combination reactions. Int. J. Chem. Kinet. 32, 118–124.

Fouchet, T., Lellouch, E., Bézard, B., Feuchtgruber, H., Drossart, P., Encrenaz, T., 2000. Jupiter's hydrocarbons observed with ISO-SWS: vertical profiles of C_2H_6 and C_2H_2, detection of CH_3C_2H. Astron. Astrophys. 355, L13–L17.

Friedson, A.J., Wong, A.-S., Yung, Y.L., 2002. Models for polar haze formation in Jupiter's stratosphere. Icarus 158, 389–400.

Gladstone, G.R., Allen, M., Yung, Y.L., 1996. Hydrocarbon photochemistry in the upper atmosphere of Jupiter. Icarus 119, 1–52.

Homann, K.H., Schweinfurth, H., 1981. Kinetics and mechanism of hydrocarbon formation in the system $C_2H_2/O/H$. Ber. Bunsenges. Phys. Chem. 85, 569–577.

Kim, S.J., Caldwell, J., Rivolo, A.R., Wagener, R., Orton, G.S., 1985. Infrared brightness of Jupiter 3. Spectrometry from the Voyager 1 IRIS experiment. Icarus 64, 233–248.

Lara, L.M., Lellouch, E., López-Moreno, J.J., Rodrigo, R., 1996. Vertical distribution of Titan's atmospheric neutral constituents. J. Geophys. Res. 101 (E10), 23,261–23,283.

Lebonnois, S., Toublanc, D., Hourdin, F., Rannou, P., 2001. Seasonal variations in Titan's atmospheric composition. Icarus 152, 384–406.

Lebonnois, S., Bakes, E., McKay, C.P., 2002. Transition from gaseous compounds to aerosols in Titan's atmosphere. Icarus 159, 505–517.

Lebonnois, S., Bakes, E., McKay, C.P., 2003. Atomic and molecular hydrogen budget in Titan's atmosphere. Icarus 161, 474–485.

Lee, A.Y., Yung, Y.L., Moses, J., 2000. Photochemical modeling of CH_3 abundances in the outer solar system. J. Geophys. Res. 105 (E8), 20207–20225.

Malkin, J., 1992. Photophysical and photochemical properties of aromatic compounds. CRC Press, Boca Raton, FL.

Marten, A., Hidayat, T., Biraud, Y., Moreno, R., 2002. New millimeter heterodyne observations of Titan: vertical distributions of nitriles HCN, HC_3N, CH_3CN, and the isotopic ratio $^{15}N/^{14}N$ in its atmosphere. Icarus 158, 532–544.

Morter, C.L., Farhat, S.K., Adamson, J.D., Glass, G.P., Curl, R.F., 1994. Rate constant measurements of the recombination reaction $C_3H_3 + C_3H_3$. J. Phys. Chem. 98, 7029–7035.

Moses, J.I., Bézard, B., Lellouch, E., Gladstone, G.R., Freuchtgruber, H., Allen, M., 2000. Photochemistry of Saturn's atmosphere. I. Hydrocarbon chemistry and comparisons with ISO observations. Icarus 143, 244–298.

Okabe, H., Becker, D.A., 1963. Vacuum ultraviolet photochemistry. VII. Photolysis of *n*-butane. J. Chem. Phys. 39 (10), 2549–2555.

Pantos, E., Philis, J., Bolovinos, A., 1978. The extinction coefficient of benzene vapor in the region 4.6 to 36 eV. J. Molec. Spectrosc. 72, 36–43.

Rages, K., Beebe, R., Senske, D., 1999. Jovian stratospheric hazes: the high phase angle view from Galileo. Icarus 139, 211–226.

Reisler, H., Mangir, M., Wittig, C., 1980. Kinetics of free radicals generated by IR laser photolysis. IV. Intersystem crossings and reactions of $C_2(X^1\Sigma_g^+)$ and $C_2(a^3\Pi_u)$ in the gaseous phase. J. Chem. Phys. 73, 2280–2286.

Schwanebeck, W., Warnatz, J., 1975. Reaktionen des butadiins. I. Die reaktion mit wasserstoffatomen. Ber. Bunsenges. Phys. Chem. 79 (6), 530–535.

Suto, M., Wang, X., Shan, J., Lee, L.C., 1992. Quantitative photoabsorption and fluorescence spectroscopy of benzene, naph- talene, and some derivatives at 106–295 nm. J. Quant. Spectrosc. Radiat. Transfer 48 (1), 79–89.

Toublanc, D., Parisot, J.P., Brillet, J., Gautier, D., Raulin, F., McKay, C.P., 1995. Photochemical modeling of Titan's atmosphere. Icarus 113, 2–26.

Vervack, Jr., R.J., 1997. Titan's upper atmospheric structure derived from Voyager ultraviolet spectrometer observations. Ph.D. thesis, Université d'Arizona.

Wang, H., Frenklach, M., 1994. Calculations of rate coefficients for the chemically activated reactions of acetylene with vinylic and aromatic radicals. J. Phys. Chem. 98, 11465–11489.

Wang, H., Frenklach, M., 1997. A detailed kinetic modeling study of aromatics formation in laminar premixed acetylene and ethylene flames. Combust. flame 110, 173–221.

Weissman, M.A., Benson, S.W., 1988. Rate parameters for the reactions of C_2H_3 and C_4H_5 with H_2 and C_2H_2. J. Phys. Chem. 92, 4080–4084.

Westmoreland, P.R., Dean, A.M., Howard, J.B., Longwell, J.P., 1989. Forming benzene in flames by chemically activated isomerization. J. Phys. Chem. 93, 8171.

Wilson, E.H., Atreya, S.K., Coustenis, A., 2003. Mechanisms for the formation of benzene in the atmosphere of Titan. J. Geophys. Res. 108 (E2), 5014.

Wong, A.-S., Lee, A.Y., Yung, Y.L., Ajello, J.M., 2000. Jupiter: Aerosol chemistry in the polar atmosphere. Astrophys. J. 534, L215–L217.

Wong, A.-S., Yung, Y.L., Friedson, A.J., 2003. Benzene and haze formation in the polar atmosphere of Jupiter. Geophys. Res. Lett. 30 (8), 1447.

Yokoyama, A., Zhao, X., Hintsa, E.J., Continetti, R.E., Lee, Y.T., 1990. Molecular beam studies of the photodissociation of benzene at 193 and 248 nm. J. Chem. Phys. 92, 4222–4233.

Yu, T., Lin, M.C., Melius, C.F., 1994. Absolute rate constant for the reaction of phenyl radical with acetylene. Int. J. Chem. Kinet. 26, 1095–1104.

Zwier, T.S., Allen, M., 1996. Metastable diacetylene reactions as routes to large hydrocarbons in Titan's atmosphere. Icarus 123, 578–583.